



HAL
open science

Nano-litter from cigarette butts: Environmental implications and urgent consideration

Quentin Chevalier, Hind El Hadri, Patrice Petitjean, Martine Bouhnik-Le Coz, Stephanie Reynaud, Bruno Grassl, Julien Gigault

► **To cite this version:**

Quentin Chevalier, Hind El Hadri, Patrice Petitjean, Martine Bouhnik-Le Coz, Stephanie Reynaud, et al.. Nano-litter from cigarette butts: Environmental implications and urgent consideration. *Chemosphere*, 2018, 194, pp.125-130. 10.1016/j.chemosphere.2017.11.158 . insu-01652616

HAL Id: insu-01652616

<https://insu.hal.science/insu-01652616>

Submitted on 30 Nov 2017

HAL is a multi-disciplinary open access archive for the deposit and dissemination of scientific research documents, whether they are published or not. The documents may come from teaching and research institutions in France or abroad, or from public or private research centers.

L'archive ouverte pluridisciplinaire **HAL**, est destinée au dépôt et à la diffusion de documents scientifiques de niveau recherche, publiés ou non, émanant des établissements d'enseignement et de recherche français ou étrangers, des laboratoires publics ou privés.

Accepted Manuscript

Nano-litter from cigarette butts: Environmental implications and urgent consideration

Quentin Chevalier, Hind El Hadri, Patrice Petitjean, Martine Bouhnik-Le Coz, Stéphanie Reynaud, Bruno Grassl, Julien Gigault



PII: S0045-6535(17)31935-5

DOI: [10.1016/j.chemosphere.2017.11.158](https://doi.org/10.1016/j.chemosphere.2017.11.158)

Reference: CHEM 20355

To appear in: *ECSN*

Received Date: 25 August 2017

Revised Date: 18 November 2017

Accepted Date: 26 November 2017

Please cite this article as: Chevalier, Q., El Hadri, H., Petitjean, P., Bouhnik-Le Coz, M., Reynaud, Sté., Grassl, B., Gigault, J., Nano-litter from cigarette butts: Environmental implications and urgent consideration, *Chemosphere* (2017), doi: 10.1016/j.chemosphere.2017.11.158.

This is a PDF file of an unedited manuscript that has been accepted for publication. As a service to our customers we are providing this early version of the manuscript. The manuscript will undergo copyediting, typesetting, and review of the resulting proof before it is published in its final form. Please note that during the production process errors may be discovered which could affect the content, and all legal disclaimers that apply to the journal pertain.

1 Nano-litter from cigarette butts: environmental implications and urgent 2 consideration

3
4 Quentin Chevalier¹, Hind El Hadri², Patrice Petitjean¹, Martine Bouhnik-Le Coz¹, Stéphanie
5 Reynaud², Bruno Grassl², Julien Gigault*¹

6
7 ¹Laboratoire Géosciences Rennes
8 CNRS-Université de Rennes 1
9 263 avenue Général Leclerc – Campus Beaulieu – Bât 15
10 35000 Rennes

11
12 ²Institut des sciences analytiques et de physico-chimie pour l'environnement et les matériaux
13 CNRS-Université de Pau et des Pays de l'Adour
14 2 avenue P. Angot – Technopôle HélioParc
15 64000 Pau

16
17
18 *Corresponding author:
19 Tel.: +33(0)223 23 53 56
20 Email: julien.gigault@univ-rennes1.fr

21 22 23 24 **Abstract** 25

26 Cigarette butts (CGB) are equivalent to plastic litter in terms of number of pieces released
27 directly into the environment. Due to their small size and social use, CGB are commonly
28 found in natural systems, and several questions have been raised concerning the contaminants
29 that are released with CGB, including metals, organic species, and nanoparticles. The aim of
30 the present study is to investigate the release of nanoscale particles from CGB by leaching
31 with rainwater. After seven days of passive stirring of both smoked and unsmoked CGB in
32 synthetic rainwater, the solutions were treated and analyzed by specific nano-analytical
33 methods. Our results demonstrate the release of $4.12 \pm 0.24\%$ (w/CGB) organic carbon in the
34 range of 10 nm up to 400 nm and with a z-average diameter of 202.4 ± 74.1 nm. The fractal
35 dimension (D_f) of the nanoscale particles ranges from 1.14 to 1.52 and suggests a soot
36 (carbon)-based composition. The analysis of some metallic species (As, Pb, Cd, Cu, Ni, Cr,
37 Co, Al, Mn, Zn, and Fe) shows that these species are essentially attached to the nanoscale

38 particles per gram of carbon released. By considering the diffusion of the nanomaterials into
39 different environmental compartments, our results suggest a new emerging and global
40 contamination of the environment by cigarette butts, comparable to plastic litter, which
41 urgently needs to be considered.

42

43 **Keywords:** Environment, Nanoparticles, Cigarette butts, Characterization, Metals

44

45

ACCEPTED MANUSCRIPT

46 1. Introduction

47 The principle litter associated with the consumption of cigarettes are smoke and cigarette
48 butts (CGB), i.e., filter compounds and cigarette smoke (Healton et al., 2011; Marah and
49 Novotny, 2011; Novotny et al., 2009). While the CO₂ contribution of cigarette smoke can be
50 considered negligible compared to that emitted by other human activities, CGB, like plastic
51 waste, raise many environmental issues. CGB are the most common form of waste found in
52 nature, and over 5.6 trillion cigarette butts can be found in nature each year (Healton et al.,
53 2011). Moreover, CGB found in the environment are likely to release their components to the
54 environment and pollute soils, water and all other environmental compartments. Several
55 studies have shown that several hazardous pollutants are released and leached from CGB,
56 which can have dramatic effects on the environmental and public health (Novotny et al.,
57 2009). Moerman and Potts highlighted the release of several metals from CGB (Cd, As, Ni,
58 Cu, Pb and Zn) with quantities ranging from few $\mu\text{g g}^{-1}$ up to several hundred $\mu\text{g g}^{-1}$
59 (Moerman and Potts, 2011), which has also been confirmed elsewhere (Dobaradaran et al.,
60 2017; Pelit et al., 2013). However, to the best of our knowledge, no data are currently
61 available concerning both their release and transport mechanisms. Recently, a new class of
62 nanoscale contaminants have been considered classified as accidental nanoparticles from
63 anthropogenic source such as nanoplastics (Koelmans et al., 2015; Ter Halle et al., 2017).
64 Due to the recent and emerging risk of nanoparticles (Baalousha et al., 2016; Bystrzejewska-
65 Piotrowska et al., 2009), questions have been raised about these new nanoscale contaminants
66 and their possible release from CGB. Recently, authors have measured the air transfer of soot
67 nanoparticles with sizes under 50 nm from the partial combustion of cigarettes into the human
68 pulmonary system (van Dijk et al., 2011). Based on this preliminary study, it is possible to
69 imagine the presence of nanoscale particles concentrated in CGB that could potentially leach
70 into the environment. According to the number of CGB released into the environment, there is

71 a considerable lack of available data on the nanoscale risk associated with CGB. The main
72 questions, therefore, are which nanoparticles (size, composition) are concentrated in CGB and
73 whether these nanoparticles are released into the environment. Due to their intrinsic
74 properties, such as size and surface area, nanoscale particles are known to transport a large
75 quantity of adsorbed species, such as metals and organic contaminants, along different
76 environmental compartments and in living organisms (Velzeboer et al., 2014; Wang et al.,
77 2013). The main concern with nanoscale particles is their ability to penetrate different natural
78 barriers to deliver the species adsorbed to their surface.

79 The aim of this paper is to demonstrate the release of nanoscale particles (NP) from cigarette
80 butts by leaching with rainwater, followed by their chemical and physical characterization.
81 Different high-resolution analytical techniques, such as in situ dynamic light scattering (IS-
82 DLS) and asymmetrical flow field-flow fractionation coupled to light scattering detection
83 (A4F-UV-SLS), were optimized for nanoscale particle characterization to measure key
84 parameters such as size distribution, aggregation information, fractal dimension, and
85 elemental composition. Our results demonstrate that a large distribution of NP sizes and
86 structures are released. The metal distribution associated with the NP fraction raised several
87 environmental concerns that urgently need to be considered. We hope that our results will
88 help tobacco control agencies to consider this type of environmental and health exposure from
89 cigarette litter.

90

91 **2. Materials and methods**

92 **2.1. Sample preparation**

93 A fresh synthetic rainwater (FSRW) sample was prepared according to Davies et al. (Davies
94 et al., 2004). Briefly, the rainwater has an ionic strength of 0.3×10^{-3} mol L⁻¹, and the
95 following components comprise 1 liter, which was then diluted by a factor of 1,000: NaNO₃,

96 4.07 g; NaCl, 3.24 g; KCl, 0.35 g; CaCl₂·2H₂O, 1.65 g; MgSO₄·7H₂O, 2.98 g; and
97 (NH₄)₂SO₄, 3.41 g. The resulting solution had a pH of 5.2. More than 12 kilograms of
98 cigarette butts (CGB) were collected over one year after immediate consumption from three
99 different places in Rennes (Brittany, France). CGB were collected directly after consumption
100 and placed directly in a plastic container under vacuum into a fridge (4°C). No CGB were
101 collected on the ground to avoid bias measurement in the leaching experiment. For a single
102 experiment, four CGB were randomly chosen, cleaned of old tobacco and placed into a 15 mL
103 conical vial (previously rinsed by HNO₃ 10% (w/v) and DI water to remove any trace of
104 HNO₃). Then, 10 mL of FSRW was added into the conical vial. Then, the vials were placed
105 on a rotator stirring at 30 rpm under classical light conditions for 7 full days. Then, the
106 leached solutions were filtered at 0.45 µm and stored in the fridge. A small fraction of the
107 solutions was kept for total metal and organic carbon analysis. The remaining volumes were
108 concentrated and size-fractionated by an ultrafiltration cell (Amicon®, Millipore, France)
109 with a 10,000 Dalton (10 kDa) molecular weight cut-off (MWCO) membrane made of
110 polyethersulfone (Nadir, Alting, Metz, France). The retentates were concentrated three times
111 and rinsed by three equivalent volumes of FSRW. The same procedure was followed for
112 unsmoked CGB (un-CGB). The CGB leaching experiments were repeated more than 5 times,
113 and the final volume was concentrated more than 20 times and rinsed 3-4 times by FSRW. All
114 experiments were repeated identically 6 times for each condition in order to obtain convenient
115 statistical results.

116

117 2.2.Reagent

118 The employed reagents were of analytical grade. The reagents to prepare the synthetic
119 rainwater and the HNO₃ used for the digestion procedure were of ultra-trace pure quality
120 (Labbox, Rungis, France). All plastic and glassware were cleaned by soaking in a 10% (w/v)

121 HNO₃ solution and then rinsed with DI water before use. All solutions were prepared using
122 ultrapure water (MilliQ, 18.2 mΩ cm).

123

124 2.3.Elemental analysis

125 Total organic carbon analysis was performed using a TOC analyzer from Shimadzu (Paris,
126 France). The metal concentrations were determined by ICP-MS using an Agilent
127 Technologies 7700x instrument. The samples were pre-digested with HNO₃ to avoid any
128 interference from organic carbon during the analysis. A flux of He was injected in a collision
129 cell to remove interferences. Quantitative analyses were performed using a conventional
130 external calibration procedure (seven external standard multi-element solutions, Inorganic
131 Venture, USA). Rhodium–rhenium was added on-line as an internal standard at a
132 concentration of 300 ppb to correct for instrumental drift and possible matrix effects.
133 Calibration curves were calculated from the intensity ratios of the internal standard and the
134 analyzed elements. The international geostandard SLRS-4 was used to control the accuracy
135 and reproducibility of the measurement procedure. The instrumental error of metal analysis
136 was below 3%. The metal concentrations in the blanks were lower than the detection limits,
137 and thus, no correction was needed.

138

139 2.4.Nanoscale particle characterization

140 In the present case, IS-DLS was used to detect the presence of nanoscale particles in the
141 aqueous system. In DLS, due to the Brownian motion of nanoscale particles, time-dependent
142 fluctuations of the scattered light intensity are measured. These fluctuations allow the
143 determination of the dynamics of the scattering particles (Burchard, 1983). The time-
144 dependent fluctuations are transformed into the auto-correlation function (ACF), which for
145 nanoscale particles in a solution, decays with a relaxation rate directly correlated to the

146 diffusion coefficient D ($\text{m}^2 \text{s}^{-1}$) and therefore, the hydrodynamic size according to the stokes-
147 Einstein equation is:

$$D = \frac{k_B T}{3\pi\eta d_H}$$

148 where d_H is the hydrodynamic diameter, η is the viscosity of the mobile phase ($\text{kg m}^{-1} \text{s}^{-1}$), T
149 is the temperature of the medium (at room temperature, 293 K) and k_B is the Boltzmann
150 constant ($1.38 \cdot 10^{-23} \text{ kg m}^2 \text{ s}^{-2} \text{ K}^{-1}$). The IS-DLS instrument used in this study is a Vasco Flex
151 from Cordouan Technologies (Pessac, France) and allows the measurement of particles
152 directly in the solution (see ESI-S1).

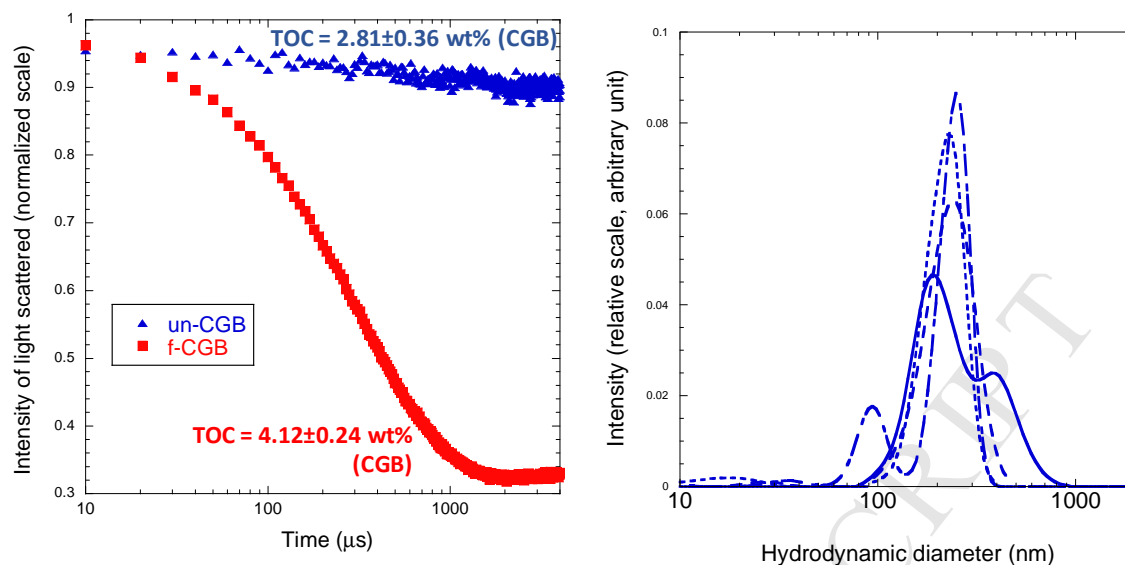
153 Asymmetrical flow field-flow fractionation (A4F), a liquid-chromatography-based
154 technique, coupled to UV-Vis and static light scattering (SLS) was used to obtain high-
155 resolution size and structure characterizations. The A4F system used in this investigation is an
156 Eclipse 3+ from Wyatt Technology (Dernbach, Germany). The trapezoidal A4F channel was
157 26.5 cm in length, 0.6 and 2.1 cm in width, and had a thickness fixed here at 250 μm . The
158 A4F fractionation conditions are optimized according to the protocol described elsewhere
159 (Gigault et al., 2014) and summarized as follows: detector flow fixed at 0.5 mL min^{-1} ;
160 relaxation flow fixed at 2.0 mL min^{-1} during 5 minutes; the elution starts with a decreasing
161 crossflow rate (exponential decay) from 2.0 to 0.1 within 40 minutes. The A4F is coupled to a
162 UV-Vis absorbance diode array detector from Agilent Technologies (Les Ulis, France) and a
163 static light scattering (SLS) detector (Dawn Heleos) from Wyatt Technology (Santa Barbara,
164 CA, USA). The SLS principle consists of measuring the intensity of light scattered by the
165 particles according to the angle of detection (Burchard, 1983). Briefly, the SLS signal
166 depends on both the concentration and size (gyration radius, R_g) of the analytes. R_g is defined
167 as the square root of the weighted average of the distance for all mass points inside a given
168 analyte (Burchard, 1983). Additionally, from SLS and the angular variation in the intensity of
169 scattered light, the fractal dimension (D_f) can be determined (Raper and Amal, 1993). With

170 regard to nanoparticles, D_f is a precise indication of both the shape and porosity of the
171 materials (see ES-S3). Discrete measurement results are reported as the mean with an
172 associated uncertainty of one standard deviation (presented as an interval or error bar) and are
173 typically based on three to five replicates performed under repeatable conditions.

174

175 **3. Results and discussion**

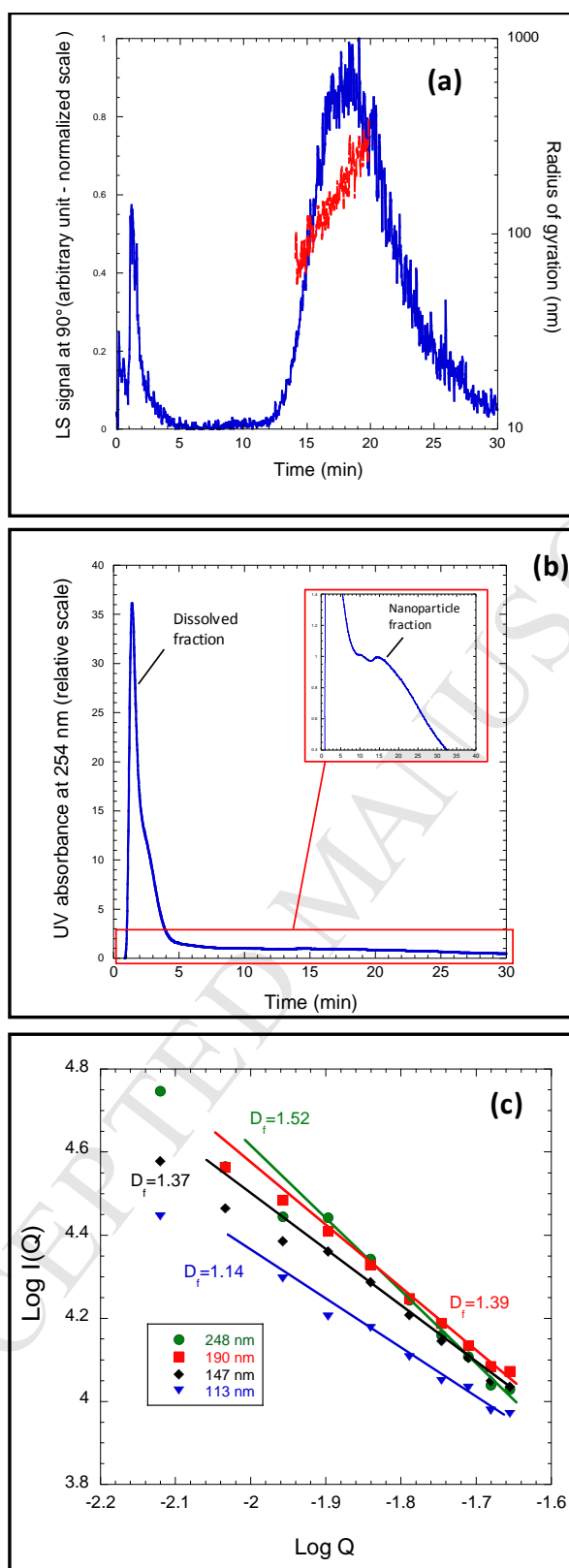
176 After the seven-day leaching experiment, the total organic carbon (TOC) in the unsmoked
177 (un-CGB) and smoked-cigarette butts (f-CGB) was measured to be $2.81 \pm 0.36\%$ (w/CGB) and
178 $4.12 \pm 0.24\%$ (w/CGB), respectively. To normalize and compare the results, the TOC values
179 are expressed as the dry weight percentage related to the total mass of CGB used in the
180 leaching experiment (w/CGB). Figure 1 presents the results obtained by IS-DLS. Even if a
181 relative quantity of TOC is released from un-CGB, no correlation in the intensity of scattered
182 light is observed in the ACF (blue dot in Fig. 1a). At this TOC concentration, a constant ACF
183 close to unity is characteristic of the absence of nanoscale particles in the solution. After
184 concentration by ultrafiltration at 10 kDa, again, correlation in the ACF is still lacking,
185 suggesting that all the carbon materials released from un-CPG are molecular and dissolved or
186 are under the size limit for DLS characterization (evaluated at 1 nm). Because cigarette filters
187 are mostly composed of cellulose-based materials, the release of these materials (degraded or
188 not) is expected (Bonanomi et al., 2015). In contrast, for f-CGB, the increase in the TOC to
189 $4.12 \pm 0.24\%$ (w/CGB) is directly correlated with the distinct exponential decay of the ACF.
190 Based on this ACF and according to the DLS theory, Figure 1b illustrates the hydrodynamic
191 diameter distribution of different leachate replicates. As expected by the filtration cut-off
192 ($0.45 \mu\text{m}$), d_H ranges from 70 to 400 nm with a maximum from 180 to 220 nm and a z-
193 average of $d_{zH} = 202.4 \pm 74.1$ nm.



194
195
196
197
Figure 1: Dynamic light scattering results of smoked and unsmoked cigarette butt leachate with (a) the autocorrelation function and (b) the corresponding size distribution of the different leaching experiments replicates. The total organic carbon (TOC) is indicated on the ACF.

198 Figure 2a and 2b presents the fractogram obtained by A4F-UV-SLS with light
199 scattering traces at 90° (Fig. 2a) and UV absorbance at 254 nm (Fig. 2b). In normal-mode
200 elution, A4F separates particles according to the coefficient of diffusion and linearly
201 according to the hydrodynamic size. The UV trace presents a large peak in the void time (at
202 lower retention time, $t_0=1$ min) corresponding to un-retained species, generally dissolved
203 species but with sizes over 10 kDa. Degraded cellulose from the cigarette filter or other small
204 molecules from the combustion process can be included in this small size fraction.
205 Additionally, in the UV trace at this void time, no size information can be obtained from SLS,
206 characteristic to particles with radii less than 10 nm (size limit of SLS detection). At higher
207 retention time (i.e., 18 minutes), the UV trace presents a second small peak relative to the
208 void time, correlated to a large and intense SLS trace. This second retained population can be
209 attributed to nanoscale particles with a smaller relative proportion than the dissolved portion.
210 This difference can be explained by the dependency of the SLS detector on both the analyte
211 concentration and size (r^6). The gyration radius (R_g) of the nanoscale particle population
212 ranges from 70 nm to 280 nm.

213 Based on both the DLS and A4F-SLS results, the maximum size determined
214 corresponds to the filtration cut-off (0.45 μm). Nevertheless, at the lower size regime, no
215 particles with sizes below 70 nm in diameter are characterized, raising several questions
216 concerning their presence and/or the limitation of the analytical methods. In a recent
217 publication, van Dijk et al. highlighted that nanoparticles with sizes ranging from 6 nm to 50
218 nm from cigarette smoke transfer to humans (van Dijk et al., 2011). Such results indicate that
219 the filters in cigarette butts cannot concentrate nanoparticles with sizes below 50 nm
220 (approximately). As demonstrated above, because sizes lower than 70 nm were not detected
221 in the CGB leachate, a hypothesis for their absence in CGB and their ability to pass through
222 the filter can be made, confirming literature data and validating our size determination results.



223
 224
 225
 226
 Figure 2: A4F analysis of nanoscale materials released from f-CGB: (a) the SLS trace and the r_G variation according to retention time, (b) the UV trace at 254 nm, and (c) the log-log plot of the scattering vector according to the intensity of the light scattered for different r_G values.

227

228

229 The correlation of the A4F-UV-SLS and IS-DLS results gives information about the
230 shape of the analytes, which can be characterized by the shape ratio expressed as R_g/r_H . Based
231 on the mean size, the R_g/r_H ratio is 1.51 ± 0.01 . This typical value is characteristic of particles
232 deviating slightly from spherical-shaped or with changing intrinsic structures. Figure 2c
233 presents the variation in the intensity of light according to the scattering vector (Q) on the log-
234 log scale (Gigault and Grassl, 2017). For $Q \times R_g > 1$, the slope is directly related to the fractal
235 dimension (D_f). Nanoscale particles released from f-CGB present highly open structures with
236 a D_f of 1.13 for 113 nm (r_G) particles up to 1.52 for $r_G=248$ nm. A D_f close to 3 corresponds to
237 spherical and compact particles and aggregates, while a D_f close to unity is characteristic of
238 one-dimensional particles, such as worm-like or other hyper-branched particles. The D_f values
239 obtained for f-CGB correspond to those obtained in previous works investigating soot
240 aggregation in aqueous system (Gorbunov et al., 1999; Luo et al., 2005; Ma et al., 2013). Due
241 to this similarity with carbon-based nanomaterials, the nanoscale particles released from CGB
242 can be hypothesized to have a soot-based composition.

243 To investigate the composition of the nanoparticle fraction and validate our previous
244 hypothesis, the leachate was ultrafiltered on a 10 kDa MWCO filter. While the filtrate (<10
245 kDa) was considered the dissolved fraction, the retentate was considered the nanoscale
246 particle fraction. The corresponding IS-DLS results are presented in the supplemental
247 information (see ES-Fig. S1). The TOC values of the two fractions are similar to those
248 obtained for the initial solutions without purification. Cigarette smoke is known to transport
249 many contaminants such as polycyclic aromatic compounds and heavy metals (Galażyn-
250 Sidorczuk et al., 2008; Järup, 2003; Luceri et al., 1993).

251

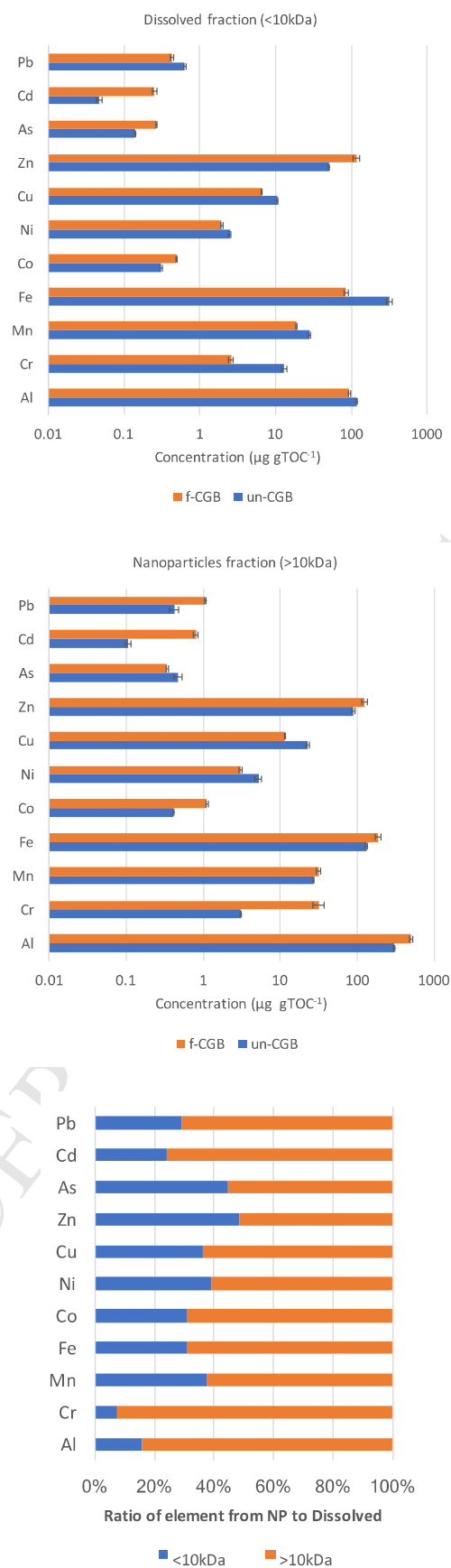
252
253
254

Figure 3: Concentration of metals per gram of organic carbon released from both the dissolved and nanoscale fractions and their relative distributions.

255

256 Figure 3 presents the variation in the principal metallic and inorganic species analyzed
257 by ICP-MS according to both the un-CGB and f-CGB fractions. To compare the results
258 among the different replicates, all concentrations in the rainwater leachate solution were
259 normalized by the amount of total organic carbon analyzed ($\mu\text{g gTOC}^{-1}$) in each fraction.
260 Among all species quantified, Fe, Al and Zn are predominant, with more than $100 \mu\text{g gTOC}^{-1}$
261 released. Cr, Mn and Cu are less dominant, with masses ranging from 1 to $50 \mu\text{g gTOC}^{-1}$
262 released. Finally, 0.1 to $1 \mu\text{g gTOC}^{-1}$ of Pb, Cd, As and Co was released. The total metal
263 concentrations are on the same order of magnitude as those reported in the literature
264 (Moerman and Potts, 2011). Considering the fractional distribution, un-CGB presents metallic
265 concentration, while no nanoparticles were identified and characterized by IS-DLS and A4F-
266 SLS. This result is explained by the low MWCO (i.e., 10 kDa) used to separate and
267 concentrate both fractions by sequential ultrafiltration. As previously explained, cigarette
268 filters are composed of cellulose-based materials (Slaughter et al., 2011). These materials are
269 degraded during the leaching process and released in a large molecular weight distribution but
270 are not sufficiently large (5-10 nm) to be detected by A4F-UV-SLS and/or DLS. For the
271 dissolved fractions, no distinct differences are observed in the metal distribution of un-CGB
272 and f-CGB. Nevertheless, for the NP fraction, except for Cu, Ni and As, an increase in metal
273 is observed. f-CGB does not show a different total amount of metal in the leached solution
274 compared to un-CGB but has a distinct effect on their distribution according to the size
275 fraction (i.e., from the dissolved to the nanoscale particle fraction). In Figure 3, the relative
276 proportion of each species characterized is illustrated according to the fraction. Except for As
277 and Zn, which are distributed equally between the two fractions, all other metal species are
278 principally distributed in the NP fraction. These results confirm the high affinity of metal
279 species with carbon-based colloids generally observed in the environment (Dai et al., 1995;

280 Hargreaves et al., 2017; Sau et al., 2010; Waeles et al., 2008). A recent work from Hargreaves
281 et al. showed that wastewater effluent contained a considerable distribution of metal (Cu, Pb,
282 Ni and Zn) in the nanoscale fraction adsorbed and/or complexed with non-humic
283 macromolecules, such as soot nanoparticles (Hargreaves et al., 2017).
284 Moreover, for Cr and Al, a clear difference is observed in that over 80% is associated with the
285 NP fraction. Alumina is known to be both in the colloidal form when in its oxide forms and
286 associated with colloid particles with fractal size distribution, such as soot particles
287 (Ringebach et al., 1995). Concerning chromium, different hypotheses are made according to
288 its oxidation state (Cr(III) or Cr(VI)) within the pH of rainwater. Soot particles are generally
289 negatively charged, and because the pH of FSRW is slightly acidic, different association can
290 be made. Further analysis to understand the precise speciation of such metals associated with
291 NP released from cigarette butts is on-going. These on-going studies concern the speciation of
292 metals according to the physical and chemical properties of the nanoscale fraction.
293 Additionally, further analyses are also planned to evaluate the stability of such nanoscale
294 particles in different environmental compartments.

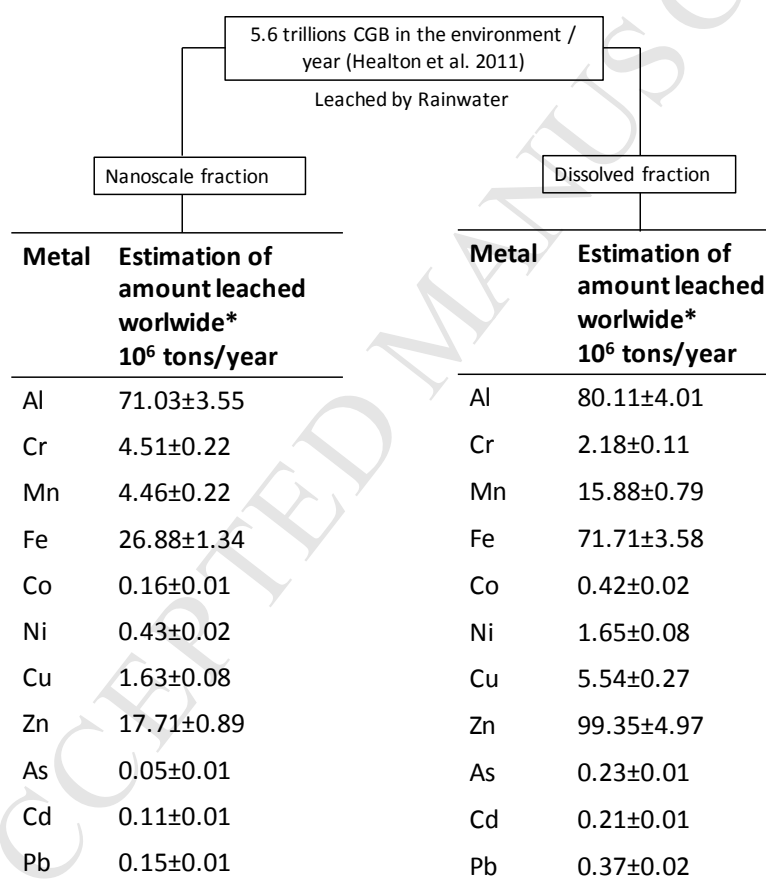
295 Without considering nanoparticles specifically, a large amount of metals is released in
296 the environment from CGB. As illustrated in Figure 4, a rapid estimation could reach several
297 millions of tons each year for both the dissolved and nanoscale fraction.

298 Currently, NP are difficult to remove in wastewater treatment plants, and most often,
299 this size fraction is directly released into the environment. Knowing the diffusion properties
300 of nanomaterials in different environmental compartments, our results suggest a new
301 emerging and global contamination of the environment by cigarette butts, comparable to
302 plastic litter, which urgently needs to be considered.

303 Indeed, compared to dissolved species (where metals can be more easily complexed,
304 accumulated and remediated), metals can be massively accumulated in the NP fraction and

305 transported over a large distance. Such transport could dramatically increase their
 306 environmental and health impacts. Slaughter et al. showed that the toxicity of cigarette butt
 307 leachate on marine and freshwater fish increased from un-CGB to f-CGB (Slaughter et al.,
 308 2011). Our results can explain this increase and suggest that by improving NP removal from
 309 wastewater combined with policies for prohibiting CGB social dumping in both urban and
 310 rural systems, an important decrease in the total amount of metal in the environment can be
 311 expected.

312



313

314 *Figure 4: Estimation of the total worldwide metal released in the environment by year from cigarette butts, according to the*
 315 *fraction considered. *The total estimation is based on the calculation of the global amount of cigarette butts littered each*
 316 *year in the environment made by Healton et al. and considers leaching from rainwater as the only release mechanism.*

317

318 Acknowledgements

319 This work is supported by “Observatoire des Sciences de l’Univers de Rennes” of the French
 320 National Center for Scientific Research (CNRS).

321

322

323 **References**

324

325 Baalousha, M., Yang, Y., Vance, M.E., Colman, B.P., McNeal, S., Xu, J., Blaszcak, J.,
326 Steele, M., Bernhardt, E., Hochella Jr., M.F., 2016. Outdoor urban nanomaterials: The
327 emergence of a new, integrated, and critical field of study. *Sci. Total Environ.* 557–558, 740–
328 753.

329

330 Bonanomi, G., Incerti, G., Cesarano, G., Gaglione, S.A., Lanzotti, V., 2015. Cigarette Butt
331 Decomposition and Associated Chemical Changes Assessed by ¹³C CPMAS NMR. *PLoS*
332 *ONE* 10.

333

334 Burchard, W., 1983. Static and dynamic light scattering from branched polymers and
335 biopolymers, in: *Light Scattering from Polymers, Advances in Polymer Science*. Springer
336 Berlin Heidelberg, pp. 1–124.

337

338 Bystrzejewska-Piotrowska, G., Golimowski, J., Urban, P.L., 2009. Nanoparticles: Their
339 potential toxicity, waste and environmental management. *Waste Manag.* 29, 2587–2595.

340

341 Dai, M., Martin, J.-M., Cauwet, G., 1995. The significant role of colloids in the transport and
342 transformation of organic carbon and associated trace metals (Cd, Cu and Ni) in the Rhône
343 delta (France). *Mar. Chem.* 51, 159–175.

344

345 Davies, C.M., Ferguson, C.M., Kaucner, C., Krogh, M., Altavilla, N., Deere, D.A., Ashbolt,
346 N.J., 2004. Dispersion and Transport of *Cryptosporidium* Oocysts from Fecal Pats under
347 Simulated Rainfall Events. *Appl. Environ. Microbiol.* 70, 1151–1159.

348

349 Dobaradaran, S., Nabipour, I., Saeedi, R., Ostovar, A., Khorsand, M., Khajeahmadi, N.,
350 Hayati, R., Keshtkar, M., 2017. Association of metals (Cd, Fe, As, Ni, Cu, Zn and Mn) with
351 cigarette butts in northern part of the Persian Gulf. *Tob. Control* 26, 461–463.

352

353 Galażyn-Sidorczuk, M., Brzóška, M.M., Moniuszko-Jakoniuk, J., 2008. Estimation of Polish
354 cigarettes contamination with cadmium and lead, and exposure to these metals via smoking.
355 *Environ. Monit. Assess.* 137, 481–493.

356

357 Gigault, J., Grassl, B., 2017. Improving the understanding of fullerene (nC60) aggregate
358 structures: Fractal dimension characterization by static light scattering coupled to
359 asymmetrical flow field flow fractionation. *J. Colloid Interface Sci.* 502, 193–200.

360

361 Gigault, J., Pettibone, J.M., Schmitt, C., Hackley, V.A., 2014. Rational strategy for
362 characterization of nanoscale particles by asymmetric-flow field flow fractionation: A
363 Tutorial. *Anal. Chim. Acta* 809, 9–24.

364

365 Gorbunov, B., Clarke, A.G., Hamilton, R.S., 1999. Coagulation of soot particles and fractal
366 dimension. *J. Aerosol Sci.* 30, S445–S446.

367

368 Hargreaves, A.J., Vale, P., Whelan, J., Constantino, C., Dotro, G., Campo, P., Cartmell, E.,
369 2017. Distribution of trace metals (Cu, Pb, Ni, Zn) between particulate, colloidal and truly

- 370 dissolved fractions in wastewater treatment. *Chemosphere* 175, 239–246.
371
- 372 Heaton, C.G., Cummings, K.M., O'Connor, R.J., Novotny, T.E., 2011. Butt really? The
373 environmental impact of cigarettes. *Tob. Control* 20, i1–i1.
374
- 375 Järup, L., 2003. Hazards of heavy metal contamination. *Br. Med. Bull.* 68, 167–182.
376
- 377 Koelmans, A.A., Besseling, E., Shim, W.J., 2015. Nanoplastics in the Aquatic Environment.
378 Critical Review, in: Bergmann, M., Gutow, L., Klages, M. (Eds.), *Marine Anthropogenic*
379 *Litter*. Springer International Publishing, pp. 325–340.
380
- 381 Luceri, F., Pieraccini, G., Moneti, G., Dolara, P., 1993. Primary Aromatic Amines from Side-
382 Stream Cigarette Smoke are Common Contaminants of Indoor Air. *Toxicol. Ind. Health* 9,
383 405–413.
384
- 385 Luo, C.-H., Lee, W.-M.G., Lai, Y.-C., Wen, C.-Y., Liaw, J.-J., 2005. Measuring the fractal
386 dimension of diesel soot agglomerates by fractional Brownian motion processor. *Atmos.*
387 *Environ.* 39, 3565–3572.
388
- 389 Ma, X., Zangmeister, C.D., Gigault, J., Mulholland, G.W., Zachariah, M.R., 2013. Soot
390 aggregate restructuring during water processing. *J. Aerosol Sci.* 66, 209–219.
391
- 392 Marah, M., Novotny, T.E., 2011. Geographic patterns of cigarette butt waste in the urban
393 environment. *Tob. Control* 20, i42–i44.
394
- 395 Moerman, J.W., Potts, G.E., 2011. Analysis of metals leached from smoked cigarette litter.
396 *Tob. Control* 20, i30–i35.
397
- 398 Novotny, T.E., Lum, K., Smith, E., Wang, V., Barnes, R., 2009. Cigarettes Butts and the Case
399 for an Environmental Policy on Hazardous Cigarette Waste. *Int. J. Environ. Res. Public.*
400 *Health* 6, 1691–1705.
401
- 402 Pelit, F.O., Demirdögen, R.E., Henden, E., 2013. Investigation of heavy metal content of
403 Turkish tobacco leaves, cigarette butt, ash, and smoke. *Environ. Monit. Assess.* 185, 9471–
404 9479.
405
- 406 Raper, J.A., Amal, R., 1993. Measurement of Aggregate Fractal Dimensions Using Static
407 Light Scattering. *Part. Part. Syst. Charact.* 10, 239–245.
408
- 409 Ringenbach, E., Chauveteau, G., Pefferkorn, E., 1995. Effect of soluble aluminum ions on
410 polyelectrolyte-alumina interaction. Kinetics of polymer adsorption and colloid stabilization.
411 *Colloids Surf. Physicochem. Eng. Asp.* 99, 161–173.
412
- 413 Sau, T.K., Rogach, A.L., Jäckel, F., Klar, T.A., Feldmann, J., 2010. Properties and
414 applications of colloidal nonspherical noble metal nanoparticles. *Adv. Mater.* 22, 1805–1825.
415 Slaughter, E., Gersberg, R.M., Watanabe, K., Rudolph, J., Stransky, C., Novotny, T.E., 2011.
416 Toxicity of cigarette butts, and their chemical components, to marine and freshwater fish.
417 *Tob. Control* 20, i25–i29.
418
- 419 Ter Halle, A., Jeannau, L., Martignac, M., Jardé, E., Pedrono, B., Brach, L., Gigault, J., 2017.

- 420 Nanoplastic in the North Atlantic Subtropical Gyre. *Env. Sci Technol* in press.
421 van Dijk, W.D., Gopal, S., Scheepers, P.T.J., 2011. Nanoparticles in cigarette smoke; real-
422 time undiluted measurements by a scanning mobility particle sizer. *Anal. Bioanal. Chem.* 399,
423 3573–3578.
- 424
425 Velzeboer, I., Kwadijk, C.J.A.F., Koelmans, A.A., 2014. Strong sorption of PCBs to
426 nanoplastics, microplastics, carbon nanotubes, and fullerenes. *Environ. Sci. Technol.* 48,
427 4869–4876.
- 428
429 Waeles, M., Tanguy, V., Lespes, G., Riso, R.D., 2008. Behaviour of colloidal trace metals
430 (Cu, Pb and Cd) in estuarine waters: An approach using frontal ultrafiltration (UF) and
431 stripping chronopotentiometric methods (SCP). *Estuar. Coast. Shelf Sci.* 80, 538–544.
432
- 433 Wang, L., Fortner, J.D., Hou, L., Zhang, C., Kan, A.T., Tomson, M.B., Chen, W., 2013.
434 Contaminant-mobilizing capability of fullerene nanoparticles (nC60): Effect of solvent-
435 exchange process in nC60 formation. *Environ. Toxicol. Chem.* 32, 329–336.
436

Highlights:

- Cigarette butts (CGB) are the most common litter found in the environment.
- This study presents new evidence of nanoscale particles (NP) leached from CGB.
- NP contain a large part of the volume of metal released from CGB.
- Our results raised urgent questions on CGB litter and their environmental impacts.